Supporting information

Long-Range Ferromagnetic Ordering in a 3D Cu^{II}-tetracarboxylate Framework Assisted by an Unprecedented Bidentate μ_2-O1,N4 Hypoxanthine Nucleobase

En-Cui Yang,* Zheng-Yu Liu, Zhong-Yi Liu, Li-Na Zhao, and Xiao-Jun Zhao*

College of Chemistry, Tianjin Key Laboratory of Structure and Performance for Functional Molecule, Tianjin Normal University, Tianjin 300387, P. R. China

Experimental Section

Materials and Instruments. All chemicals were commercially purchased (HypH and H_4btec were from Acros and other analytical-grade reagents were from Tianjin Chemical Reagent Factory) and used as received without further purification. Powder X-ray diffraction (PXRD) patterns were obtained from a Rigaku D/max-2500 diffractometer at 60 kV and 300 mA for Cu *K*α radiation (λ = 1.5406 Å), with a scan speed of 2 deg/min and a step size of 0.02^{o} in 2θ. The simulated PXRD patterns were calculated using single-crystal X-ray diffraction data and processed by the free *Mercury v1.4* program provided by the Cambridge Crystallographic Data Center. Elemental analyses for C, H, and N were carried out with a CE-440 (Leeman-Labs) analyzer. Fourier transform (FT) IR spectra (KBr pellets) were taken on an Avatar-370 (Nicolet) spectrometer in the range 4000 – 400 cm^{-1}. Thermogravimetric analysis (TGA) experiments were performed on Shimadzu simultaneous DTG-60A compositional analysis instrument from room temperature to 800 ^{o}C under N_2 atmosphere at a heating rate of 5 ^{o}C min^{-1}. Magnetic susceptibilities were acquired on a Quantum Design (SQUID) magnetometer MPMS-XL-7 with phase-pure crystalline samples. The data were corrected for TIP and the diamagnetic corrections were calculated using Pascal's constants. And an experimental correction for the sample holder was also applied.

Table S1. Selected bond lengths /Å and angles /° for **1** [a]

Cu(1)–O(7)[a]	1.923(2)	Cu(3)–O(6)	1.929(3)
Cu(1)–O(8)[b]	1.925(2)	Cu(3)–O(3)[d]	1.933(3)
Cu(1)–O(1)	2.219(3)	Cu(3)–O(9)[e]	1.939(2)
Cu(2)–O(2)	1.952(2)	Cu(3)–O(5)[f]	1.960(2)
Cu(2)–O(4)[c]	1.987(2)	Cu(3)–O(10)	2.580(0)
Cu(2)–N(4)	2.227(4)		
O(7)[a]–Cu(1)–O(7)[b]	87.54(15)	O(4)–Cu(2)–O(4)[c]	89.16(12)
O(7)[a]–Cu(1)–O(8)[b]	175.46(10)	O(2)[c]–Cu(2)–N(4)	113.11(9)
O(7)[a]–Cu(1)–O(8)[a]	91.55(11)	O(4)–Cu(2)–N(4)	90.48(9)
O(8)[b]–Cu(1)–O(8)[a]	89.01(16)	O(6)–Cu(3)–O(3)[d]	174.40(11)
O(7)[a]–Cu(1)–O(1)	93.31(9)	O(6)–Cu(3)–O(9)[e]	90.67(10)
O(8)[a]–Cu(1)–O(1)	91.18(9)	O(3)[d]–Cu(3)–O(9)[e]	90.76(11)
O(2)–Cu(2)–O(2)[c]	84.72(12)	O(6)–Cu(3)–O(5)[f]	88.20(9)
O(2)–Cu(2)–O(4)	88.26(9)	O(3)[d]–Cu(3)–O(5)[f]	90.78(10)
O(2)–Cu(2)–O(4)[c]	156.28(9)	O(9)[e]–Cu(3)–O(5)[f]	175.53(10)

[a] Symmetry codes: [a] $x + 1/2, -y + 1, z - 1/2$, [b] $-x + 3/2, -y + 1, z - 1/2$, [c] $-x + 2, y, z$, [d] $x, y, z + 1$, [e] $-x + 3/2, -y + 1, z + 1/2$, [f] $-x + 3/2, -y, z + 1/2$.

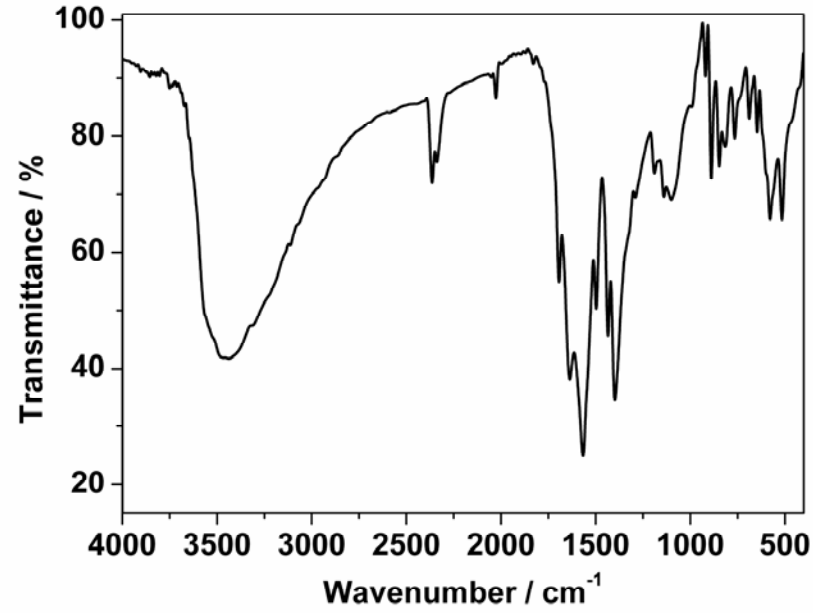

Fig. S1 FT-IR spectrum of complex **1**.

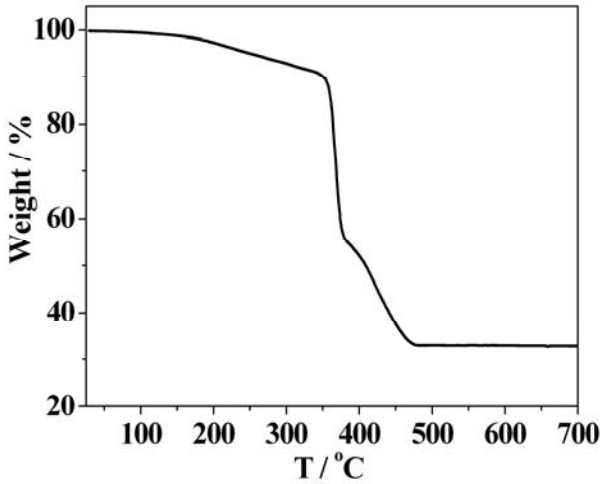

Fig. S2 TG curve for **1**.

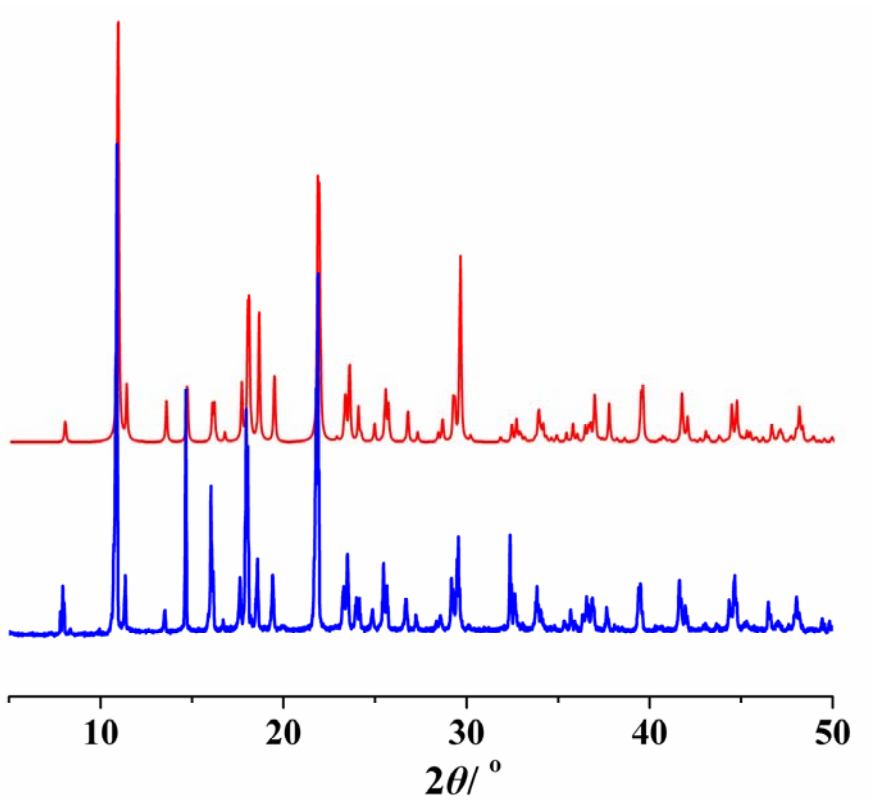

Fig. S3 Calculated (red) and experimental (blue) X-ray powder diffraction patterns for **1**.

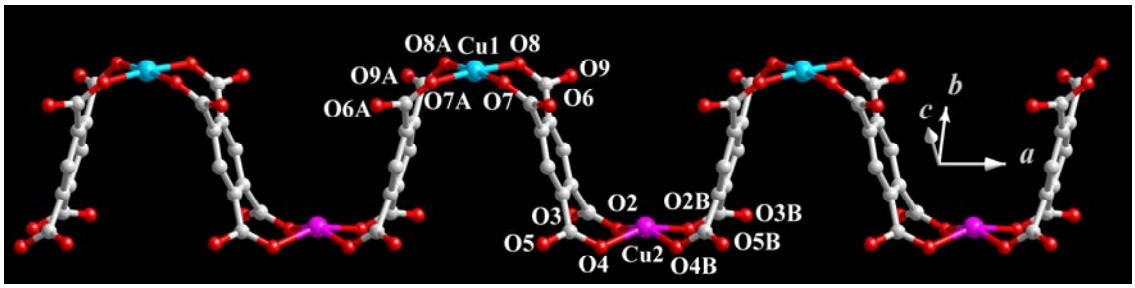

Fig. S4 The alternate head-to-head and tail-to-tail arrangements of btec^{4-} ligands in Cu-btec ribbon.

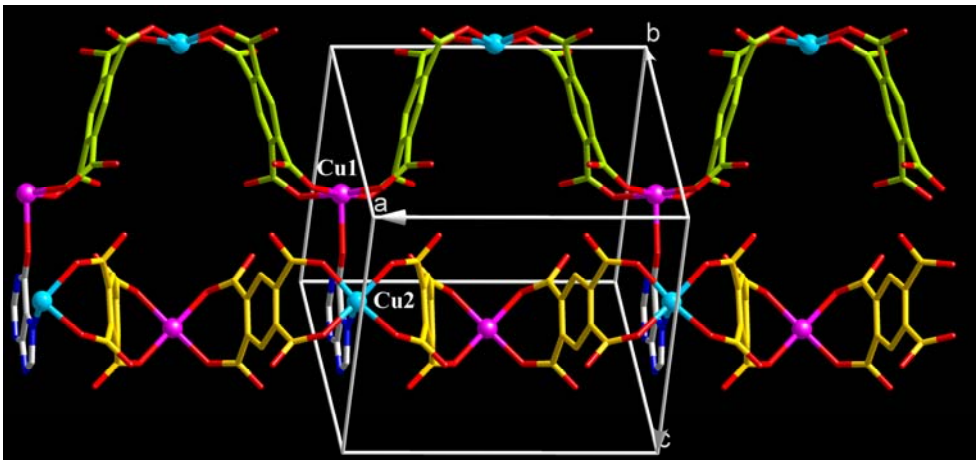

Fig. S5 Two adjacent Cu-btec chains propagated along two perpendicular directions.